A combined LC-MS and NMR approach to reveal metabolic changes in the hemolymph of honeybees infected by the gut parasite Nosema ceranae

Cyril C. Jousse, Céline Dalle, Angélique Abila, Mounir Traïkia, Marie Diogon, Bernard Lyan, Hicham El Alaoui, Cyril Vidau, Frédéric Delbac

▶ **To cite this version:**

Cyril C. Jousse, Céline Dalle, Angélique Abila, Mounir Traïkia, Marie Diogon, et al.. A combined LC-MS and NMR approach to reveal metabolic changes in the hemolymph of honeybees infected by the gut parasite Nosema ceranae. Journal of Invertebrate Pathology, 2020, 176, pp.107478. 10.1016/j.jip.2020.107478 . hal-03132817

HAL Id: hal-03132817
https://hal.uca.fr/hal-03132817

Submitted on 17 Oct 2022

HAL is a multi-disciplinary open access archive for the deposit and dissemination of scientific research documents, whether they are published or not. The documents may come from teaching and research institutions in France or abroad, or from public or private research centers.

L'archive ouverte pluridisciplinaire **HAL**, est destinée au dépôt et à la diffusion de documents scientifiques de niveau recherche, publiés ou non, émanant des établissements d'enseignement et de recherche français ou étrangers, des laboratoires publics ou privés.

Distributed under a Creative Commons Attribution - NonCommercial| 4.0 International License

Version of Record: https://www.sciencedirect.com/science/article/pii/S0022201120301841
Manuscript_d20e65e1f9f0703623ee0026463d29f4

1 **Title**

2 A combined LC-MS and NMR approach to reveal metabolic changes in the hemolymph of
3 honeybees infected by the gut parasite *Nosema ceranae*

4 Authors : Cyril Jousse[2,3*], Céline Dalle[2,3], Angélique Abila[2,3], Mounir Traikia[2,3], Marie Diogon[1],
5 Bernard Lyan[2,3], Hicham El Alaoui[1], Cyril Vidau[4], Frédéric Delbac[1]

6

7 [1] Université Clermont Auvergne, CNRS, Laboratoire "Microorganismes : Génome et
8 Environnement", F-63000 Clermont–Ferrand, France.

9 [2] Université Clermont Auvergne, CNRS, Sigma-Clermont, Institut de Chimie de Clermont-
10 Ferrand, F-63000, Clermont-Ferrand, France.

11 [3] Plateforme d'Exploration du Métabolisme, Université Clermont Auvergne & I.N.R.A site de
12 Theix, Clermont-Ferrand, France.

13 [4] ITSAP, UMT PrADE, Inra – Acta, 228 route de l'aérodrome, F-84000, Avignon, France
14 (current address).

15

16 [*] Corresponding author.

17 Email: cyril.jousse@uca.fr; Address: Institute of Chemistry of Clermont-Ferrand, 24 avenue
18 Blaise Pascal, 63178 Aubière cedex, France

19

20 **Highlights**

21 * Honeybee hemolymph metabolome is altered by the gut parasite *Nosema ceranae*

22 * 15 metabolites were identified by LC-MS and NMR as candidate biomarkers of infection

23 * Putative biomarkers are involved in carbohydrate, amino acid and lipid metabolic
24 pathways

© 2020 published by Elsevier. This manuscript is made available under the CC BY NC user license
https://creativecommons.org/licenses/by-nc/4.0/

Abstract

Nosema ceranae is an emerging and invasive gut pathogen in *Apis mellifera* and is considered as a factor contributing to the decline of honeybee populations. Here, we used a combined LC-MS and NMR approach to reveal the metabolomics changes in the hemolymph of honeybees infected by this obligate intracellular parasite. For metabolic profiling, hemolymph samples were collected from both uninfected and *N. ceranae*-infected bees at two time points, 2 days and 10 days after the experimental infection of emergent bees. Hemolymph samples were individually analyzed by LC-MS, whereas each NMR spectrum was obtained from a pool of three hemolymphs. Multivariate statistical PLS-DA models clearly showed that the age of bees was the parameter with the strongest effect on the metabolite profiles. Interestingly, a total of 15 biomarkers were accurately identified and were assigned as candidate biomarkers representative of infection alone or combined effect of age and infection. These biomarkers included carbohydrates (α/β glucose, α/β fructose and hexosamine), amino acids (histidine and proline), dipeptides (Glu-Thr, Cys-Cys and γ-Glu-Leu/Ile), metabolites involved in lipid metabolism (choline, glycerophosphocholine and O-phosphorylethanolamine) and a polyamine compound (spermidine). Our study demonstrated that this untargeted metabolomics-based approach may be useful for a better understanding of pathophysiological mechanisms of the honeybee infection by *N. ceranae*.

Keywords: Honeybee; Metabolomic; *Nosema ceranae*; Stress Biomarkers

1. Introduction

48 Honeybees provide essential ecosystem services in agricultural and natural areas by
49 pollinating many crops and native plants. However, these insect pollinators are exposed to
50 multiple abiotic (pollutants, pesticides) and biotic (infectious agents, parasites) stressors
51 which are detrimental to their health and lifespan. Among them, both parasites and
52 pesticides seem to be the most important stressors affecting honeybees and contribute to
53 the decline of their populations (Goulson et al., 2015; vanEngelsdorp et al., 2009;
54 vanEngelsdorp and Meixner, 2010).
55
56 The gut parasite *Nosema ceranae* is among the most common pathogens in *Apis mellifera*,
57 with a worldwide distribution (Goulson et al., 2015) and is now considered to be a major
58 threat to the Western honeybee at both the individual and colony levels (Fries, 2010; Higes
59 et al., 2013; Paris et al., 2018; vanEngelsdorp and Meixner, 2010). Similar to other
60 microsporidian species, *N. ceranae* can alter the bee physiology and behavior in order to
61 maintain a more favorable environment for its reproduction. Several studies have
62 demonstrated that *N. ceranae* infection impairs tissue integrity in the midgut (Dussaubat et
63 al., 2012), alters the energy demand in honey bees (Alaux et al., 2009; Martín-Hernández et
64 al., 2011; Mayack and Naug, 2009; Naug and Gibbs, 2009) and decreases hemolymph sugar
65 level (Mayack and Naug, 2010). The infection also significantly suppresses the bee immune
66 response (Alaux et al., 2009; Antúnez et al., 2009; Aufauvre et al., 2014; Chaimanee et al.,
67 2012; Dussaubat et al., 2012) and alters pheromone production in worker and queen honey
68 bees (Alaux et al., 2011; Dussaubat et al., 2010; Holt et al., 2013). Some studies also revealed
69 that *N. ceranae*-infected honeybees have shorter lifespans than uninfected honeybees
70 (Alaux et al., 2009; Goblirsch et al., 2013; Higes et al., 2006; Vidau et al., 2011). However, the
71 presence of *N. ceranae* is not systematically associated with honeybee weakening and

mortality (Cox-Foster et al., 2007; Gisder et al., 2010; Invernizzi et al., 2009), suggesting modulations in the parasite virulence. Possible explanations for this variation include parasite or host genetics (Chaimanee et al., 2010; Dussaubat et al., 2013; Medici et al., 2012; Williams et al., 2008), climate (Chen et al., 2012; Gisder et al., 2010), nutrition (Alaux et al., 2010b; Fleming et al., 2015), or interactions with other stressors such as environmental contaminants or other parasites. Indeed, some recent studies demonstrated that *N. ceranae* can sensitize the honeybees to chemical stressors (Alaux et al., 2010a; Aufauvre et al., 2014, 2012; Pettis et al., 2012; Retschnig et al., 2014; Vidau et al., 2011; Wu et al., 2012).

In order to explain disorders and detect (early) modifications on bee physiology, we must acquire molecular tools to screen from genome to metabolome (Lankadurai et al., 2013). Among these tools, metabolomics is the most informative, looking at the end of the "omic cascade" for the small metabolites, and strongly linked to the phenotype (Alonso et al., 2015; Bundy et al., 2008; Fiehn, 2002; Liu and Locasale, 2017). Most of the time, to visualize a wide range of metabolites, several analytical techniques are required. Mass spectrometry (MS) is one of the most sensitive and precise technique, depending on mass spectrometer accuracy, but is limited by chromatographic coupling and in-source ionization. Nuclear magnetic resonance (NMR) spectroscopy provides the widest coverage of all techniques. Nevertheless, sensitivity and resolution are regular drawbacks.

Untargeted metabolomics has the advantage to highlight both known and unknown metabolites resulting from phenotypic evolution. Based on statistical filters, all signals from analytical devices (MS and/or NMR) are examined for possible correlation with the observed biological effect (Wishart et al., 2008). Those with high correlation will be submitted to deeper analyses as data/base mining, MS-MS and/or 2-dimensional NMR experiments if needed, to reveal the identity of the associated biomarker.

One of the most established protocols in metabolomics is the metabolic profiling of plasma (Simón-Manso et al., 2013; Zhao et al., 2010) and urine (Zhang et al., 2012) on "higher animals". Biological fluids are easy to collect and store and contain a wide range of metabolites that can be impacted by many physiological disturbances including medication, nutrition or disease (Zhang et al., 2020). In this way, researchers aim to find host biomarkers for early diagnosis of infectious diseases, collect evidence of metabolic disorders along time-periods or improve nutrition benefits. Hemolymph is the sole biofluid in the insect, analogous to the blood in invertebrates, and is composed of fluid plasma in which hemolymph cells (hemocytes) are suspended. It circulates in the interior of the insect body and remains in direct contact with the animal's tissues. Analyzing this fluid is an opportunity to access to metabolic pool impacted by stressors (Aliferis et al., 2012; Wang et al., 2019). Aliferis et al. (2012) previously reported by GC/MS the metabolite profiling of hemolymph in bees naturally infected by *N. ceranae*. They revealed that a gut parasite can induce a general disturbance of the honeybee physiology.

In our study, we have developed a methodology to perform metabolomics on hemolymph samples, using combined LC/MS and NMR approaches. The aim was to investigate the metabolic response of honeybees following experimental infection of emergent bees by *N. ceranae*. Metabolome of the hemolymph was examined in both infected and uninfected honeybees at two post-infection times.

2. Materials and methods

2.1. Biological experiments

2.1.1. Honeybee artificial rearing

All experiments were performed with a mixture of honeybees taken from three Buckfast colonies of the same apiary at the Laboratoire Microorganismes : Génome et Environnement (UMR 6023, Université Clermont Auvergne, France). We confirmed that the three colonies were free of *Nosema* (sampling of 30 foragers for each colony) by PCR using specific primers as previously described (Higes et al., 2006). Two frames of sealed brood were placed in an incubator in the dark at 33°C with 60% relative humidity. Emerging honeybees (100 per colony) were collected, confined to laboratory Pain-type cages in two groups (infected *vs* uninfected, see below for the infection procedure) of 50 individuals, and maintained in the incubator. During this time, honeybees were fed *ad libitum* with candy (Apifonda®) supplemented with fresh pollen (Naturapi). In order to mimic the colony environment, a small piece of wax and a 5-mm piece of Beeboost® (Pherotech, Delta, BC, Canada) releasing five queen mandibular pheromones, were placed in each cage. Each day, feeders were replaced; dead bees were counted and removed.

2.1.2. Experimental infection with Nosema ceranae

Spores of *N. ceranae* were obtained from bees experimentally-infected in the laboratory and the infection process was conducted as previously described (Vidau et al., 2011). Briefly, the intestinal tract of infected bees was dissected and homogenized in PBS and the resulting suspension was filtered through Whatman No 1 filter paper, cleaned by centrifugation and resuspended in PBS. At 5 d post-emergence, caged honeybees were starved for 3 h, CO_2-anaesthetized and individually transferred in ‘‘infection boxes’’ consisting of 40 ventilated compartments (3.5 cm^3). Each compartment was supplied with a tip containing 125,000 spores of *N. ceranae* diluted in 3 µL of water. ‘‘Infection boxes’’ were placed in the incubator

144 and 1 h later, bees that had consumed the total spore solution were again caged (50 bees per
145 cage). Uninfected bees were similarly treated without *N. ceranae* spores in the water. At the
146 end of the experiment, we checked that the control remained uninfected.
147
148 ***2.1.3. Hemolymph sampling***
149 Hemolymph samples were collected at day 2 (D2) and day 10 (D10) post-inoculation from
150 both infected and control (uninfected) honeybees using the method described by (Mayack
151 and Naug, 2010). Bees were first CO_2-anaesthetized and placed on ice, before antenna
152 cutting. Immediately, honeybees were placed into PCR tube and centrifuged at 16,000 x *g*
153 during 30 s. Hemolymph was collected in a new tube and stored at -80°C until analysis.
154
155 ***2.2. Chemical analyses***
156
157 ***2.2.1. Chemicals and reagents***
158 Creatinine (Fluka), phenylalanine and tryptophan (Sigma-Aldrich) were used as external
159 standards for LC/MS quality control. For NMR experiments, Deuterium oxide (D_2O) was
160 purchased from Eurisotop and 3-(trimethylsilyl) propionic-2,2,3,3- tetra-d_4 acid sodium salt
161 (TSP-d_4) was purchased from Sigma-Aldrich. Acetonitrile (Optima LC-MS), water (Optima LC-
162 MS) and ammonium acetate (Optima) were purchased from Fisher Scientific for LC/MS
163 analyses. MS external calibration was performed using lithium hydroxide monohydrate and
164 formic acid (Fluka).
165
166 ***2.2.2. Standard solutions and sample preparations for LC/MS and NMR***
167 Stock solutions were prepared for each standard compound (creatinine, phenylalanine and

tryptophan) at a concentration of 0.5 mg/ml in water/acetonitrile 1:1 containing 0.1% formic acid and were stored at -20°C. A mix of all standard solutions was extemporaneously prepared, for a final concentration of 5 µg/mL. Repeated analyses of the mixed standard solution ensure system stability before analysis of biological samples. Forty-eight hemolymph samples (10 µL each, 12 per modality) were diluted in water (LC/MS grade) 1:4 to decrease viscosity and provide a sufficient volume, considering LC sampling capabilities. Finally, 5 µL was injected in LC/MS for each analysis. For ^{1}H-NMR analyses, 51 hemolymph samples (12 bees per modality, but 15 for infected ones at D10) were centrifuged at 14000 x *g* for 10 min at 4°C. Three hemolymph samples (from the same experimental condition) were pooled (to reach the minimum volume required for NMR experiment) and the final volume was adjusted to 50 µl with D_2O. The Metabolic Profiler® platform robot (Bruker) prepared all analytical samples by mixing 50 µl of pooled samples with 150 µl of phosphate buffer (1.5 M phosphate in D_2O at pH 7.06). D_2O was used for shimming and locking, whereas TSP-d_4 constituted a reference for chemical shifts (0 ppm) for NMR. Finally, 180 µl of the solution was injected, through a capillary, for the online ^{1}H-NMR profiling. Quality control samples were also prepared using aliquots from each analytical sample. They ensure system stability and permit to improve spectra processing.

2.2.3. Metabolic profiler® platform (Bruker Biospin, France)

Ultraperformance liquid chromatography-mass spectrometry (UPLC-MS) used was a MicroToF system (Bruker) equipped with an electrospray ionization probe (ESI) and a 1200 series chromatographic system (Agilent). Chromatographic separation was performed with a kinetex HILIC column (100 x 2.1mm, 2.6 µm, Phenomenex) with pre-column. The mobile phase was composed with acetonitrile (A) and water (B) solvents, both containing 10 mM

192 ammonium acetate. The flow rate was 0.4 mL/min and the gradient elution was carried out
193 as follows: 0-2 min at 100% A; 2-4 min linear gradient to 80% A; 4-13 min linear gradient to
194 20% A and back to 100% A into 10 sec (initial conditions); 1 min 50 sec equilibration wash
195 with 100% A, for a total run of 15 min. The injection volumes for both samples and standards
196 were 5 µL and the column temperature was set at 25°C. Blanks of pure water and pure
197 acetonitrile were injected after every 10 hemolymph samples, for cleaning the
198 chromatographic system. The mass spectrometer was calibrated with lithium formate
199 clusters (5 mM into water) and operated in positive ion mode for full scan (50-1000 m/z)
200 detection. Nitrogen was used as the nebulizer and the drying gas. The nebulizer pressure was
201 2 bars, the desolvation gas flow rate was 8 L/min and desolvation temperature was
202 maintained at 200°C. Capillary tension was 4000 V.
203 On flow 1-dimensional ^{1}H-NMR experiments were done on an Avance III 500 MHz NMR
204 spectrometer, using an inflow 3-mm FISEI z-gradient (1H-13C) probe with a 60-µl cell.
205 A standard one dimensional noe spectroscopy sequence (noesygppr1d with water
206 presaturation and gradients) was used with low power irradiation of the water resonance
207 during the recycle delay of 4 s and the mixing time of 10 ms. 256 scans were collected with
208 an 90° impulsion time of 9.29 µs, an acquisition time of 3.28 s, a spectral window of 10000
209 Hz and 64K data points zero-filled to 128K before Fourier transformation with 0.3 Hz line
210 broadening. All NMR spectra were recorded at 300K and processed with Topspin version 2.1.
211
212 ***2.2.4. Ultraperformance liquid chromatography-tandem mass spectrometry (UPLC-MS-MS)***
213 For identification purposes, a few samples from each condition, and that were representative
214 for the features in the model, were analysed in full scan (80-1000 m/z) for positive ion mode
215 on an LTQ Orbitrap Velos MS with same chromatographic conditions (gradient, column) as for

UPLC-MS profiling. The m/z of each feature was searched in the resulting chromatograms to obtain a better mass accuracy of the features, which was used to determine the most probable molecular formulae. The parent ion was identified from in-source fragments and adducts, and additional structural information on the features was obtained by performing MS/MS fragmentation on relevant ions using MS-MS in product ion scan mode with collision energies of 10, 20, and 30 eV. All information on the features was used to search into chemicals and metabolites databases (cf. § 2.5.3).

2.2.5. 1D and 2D NMR experiments for metabolite identification

For the metabolite identification step, the sample corresponded to a pool of 25 hemolymphs (mix of both infected and uninfected bees). The total volume of hemolymph (300 µl) was mixed with 300 µl of phosphate buffer in D_2O. The NMR spectrometer used (TGIR - CNRS de Gif/Yvette) was a Bruker Avance III 950 MHz equipped with a cryoprobe (1.7, 3 and 5 mm tube) TCI ($^{1}H/^{13}C/^{15}N/^{2}H$) with z-gradient coil probe (Bruker Biospin Wissenbourg, France). For 1D ^{1}H-Spectra, a standard one dimensional noe spectroscopy sequence (noesygppr1d with water presaturation and gradients) was used with low power irradiation (31 µW) of the water resonance during the recycle delay of 10 s and the mixing time of 10 ms. 128 scans were collected with a 90° impulsion time of 8.1 µs, an acquisition time of 3.3 s, a spectral window of 10000 Hz and 64K data points zero-filled to 128K before Fourier transformation with 0.3 Hz line broadening. For 2D homonuclear (COSY TOCSY, JRES) and heteronuclear ($^{1}H/^{13}C$ HSQC and HMBC) experiments were performed with quadrature phase detection in dimensions, using state-TPPI or QF detection mode in the indirect one. For each 512 (80 for JRES) increments in the indirect dimension, 2K data points (8K for JRES) were collected and 16 transients were accumulated in the direct dimension. ^{13}C decoupling (GARP) was

performed during acquisition time for heteronuclear experiments. A π/2 shifted square sine-bell function was applied in the two dimensions before Fourier transformation. Spectra were treated with Topspin version 3.1. All NMR spectra were recorded at 300K.

2.3. Data management

2.3.1. Data extraction

MS data were converted into NetCDF format and extracted to data matrix using XCMS package under R environment (v. 2.15.3). Briefly, after ion extraction (m/z), a retention time (RT) correction was performed before production of the matrix including for each ion (m/z@RT) the relative intensity (area) detected into each analytical sample. Finally, CAMERA package (Kuhl et al., 2012) proposed a first annotation according to common adducts and natural isotopes. NMR data were binned using AMIX software (v. 3.9.10, Bruker) after alignment and baseline correction. Extraction process was chosen as follows: fixed bucketing of 0.01 ppm, from 0.13 to 10 ppm; solvent signal exclusion between 4.7 and 4.9 ppm; signals integration on the sum of intensities; normalization on total intensity. The resulting matrix was used for statistics.

2.3.2. Statistical analyses

Multivariate analyses were performed using SIMCA-P+ (v. 12.0.1.0, Umetrics) for non-supervised (PCA) and supervised ((O)PLS-DA) methods. Two normalization methods were tested, univariate (UV) and pareto (PAR), in order to obtain the most robust statistical models. All statistical models were validated according to explanatory (R^2) and predictive (Q^2) values as well as with random permutations. Lists of signals (ions or buckets) were

selected for each model according to VIP (variable importance in projection) scores (>1). For all valid models, a list of ions considered to be the most implicated was selected, according to VIP score. Univariate analyses were performed on Excel software (Windows) for ANOVA filtering on MS data. ANOVA multiway, with interaction, was performed in order to separate analytical effects from biological ones and to distinguish, when possible, age and infection metabolic effects.

2.3.3. Metabolite identification

Identification of VIP ions was performed manually or using R script for data mining on several public metabolic databases (KEGG, MetaCyc, HMDB). MS-MS fragmentation features were compared to MassFrontier (v. 7; ThermoScientific) theoretical schemes and databases (MassBank, METLIN, HMDB, PRIMe). NMR VIP signals (buckets) were attributed manually using previously published data (Fan, 1996; Nicholson et al., 1995; Willker et al., 1996) and the human metabolome public database (HMDB).

3. Results

For metabolic profiling, hemolymph samples from both uninfected (UI) and *N. ceranae*-infected (I) bees were collected at two time points considered as early (D2) and late (D10) times of infection, respectively. Forty eight samples (12 for each modality) were individually analyzed by LC-MS in two batches (23 samples for batch 1 and 25 samples for batch 2). For ^{1}H-NMR experiments, hemolymph from 51 bees were pooled in 17 groups of three.

3.1. LC-MS profiles and metabolite identification

All hemolymph samples analyzed by LC-MS showed similar “total ion chromatogram” profiles (**Suppl. Fig. 1**). Multivariate models were then applied to measure age (D2 *vs* D10) and treatment (I *vs* UI) effects from a data matrix of 1294 ions. Among each analytical batch, PLS-DA models clearly showed that the age of bees remained the parameter with the strongest effect (**Figure 1**) and no statistical model was valid considering the infection effect only. ANOVA filtering permitted discrimination between batch effect and combined effect of age and infection, and all ions with a p-value above 0.05 were eliminated. A final list of 15 ions according to VIP scores, with levels significantly up- or down-regulated (at D2 and/or D10), was then used for metabolite identification. Eight metabolites, corresponding to potential biomarkers representative of infection alone or combined effect of age and infection, were accurately identified according to spectral data and/or standard comparisons (**Table 1**). These biomarkers included 3 dipeptides (Glu-Thr, Cys-Cys and γ-Glu-Leu/Ile), one amino acid (histidine), one amino sugar (hexosamine), two metabolites involved in lipid metabolism (glycerophosphocholine and O-Phosphorylethanolamine) and ethyl aconitate, a tricarboxylic acid derivative, listed as flavoring agent. For each selected marker, infected/uninfected (I/UI) ratios were mentioned at both D2 and D10 post-infection times. The most interesting metabolite was hexosamine. In hemolymph of infected bees, the circulating amount of hexosamine was 3x lower at D2 and 7-8x higher at D10 compared to the control (**Table 1**). Similarly, in infected bees compared to control, levels of circulating histidine and another “amino acid-like” putative compound were lower at D2 and higher at D10. Three other metabolites (glycerophosphocholine and two dipeptides, Cys-Cys and Glu-Thr) exhibited an opposite pattern. These circulating metabolites were more abundant at D2 and lower at D10. O-phosphorylethanolamine, a “sulfur-containing” putative metabolite and peptides (γ-Glu-Leu/Ile and another putative “short peptide”) were detected at higher levels

311 in the hemolymph of infected bees at D2 and D10. Finally, ethyl aconitate, levels of
312 circulating “carbohydrate-like” and “amine-like” putative compounds were lower in infected
313 bees than in control bees, at the two time points post-infection.
314
315 ***3.2. NMR profiles and metabolite identification***
316 Each NMR spectrum was obtained from a pool of hemolymphs from three honeybees.
317 Spectra analysis showed signal richness of both aliphatic and sugar zones, below 5 ppm
318 (**Suppl. Fig. 2**). Using multivariate statistical analysis tools, we observed a strong effect of
319 ageing with PCA and PLS-DA models (**Figure 2**). Similar to MS results, age had the strongest
320 effect and no valid model was obtained when considering the infection parameter alone.
321 Buckets were selected according to VIP score (above 0.99). Eight biomarkers were clearly
322 identified, according to spectral data and databases comparisons, and I/NI ratios were
323 calculated at both D2 and D10 (**Table 2**). These biomarkers included four carbohydrates
324 (fructose and glucose, both α and β forms), one amino acid (proline), a polyamine compound
325 (spermidine) and two metabolites involved in lipid metabolism (choline and
326 glycerophosphocholine). Signals for carbohydrates (fructose and glucose) shared similar
327 behaviors. These compounds were more abundant in the hemolymph of infected bees
328 particularly at the early infection time (D2). In contrast, proline was always less abundant in
329 infected hemolymph. As for the MS data, levels of circulating glycerophosphocholine were
330 higher in the hemolymph of infected bees at D2, then decreased at D10. Choline showed a
331 completely opposite pattern. Although the amount of spermidine decreased at D2 for
332 infected bees, no significant difference was observed at D10 between I and UI samples.
333
334 ***4. Discussion***

335

336 ***4.1. Biological sampling***

337 This proof of concept study was performed to develop transposable methodologies for
338 metabolic profiling on honeybee hemolymph from bees in hives and was linked to a study of
339 experimental infection of caged honeybees by the gut parasite *N. ceranae* conducted to
340 reveal metabolic shifts during the infectious process. We also raised several questions about
341 the quality and variability of biological samples.

342 Experimental results have suggested difficulties in assessing the health status of honeybees
343 from hives in field conditions. Both biotic and abiotic stressors may produce effects on the
344 physiology of the bees and modify the metabolic pool. Even using molecular biology (RNA
345 seq and/or qPCR) and analytical (multiresidue detection) tools, it is too time consuming and
346 costly to evaluate unstressed bees (*i.e.* healthy bees). Only visual symptoms and mortality
347 were evaluated during the experiment. In our opinion, difficulty in obtaining clear signatures
348 of *Nosema* infection in natural populations are partly due to honeybee genetic variability.
349 For example, Kurze et al. (2015) demonstrated that *Nosema*-tolerant honeybees were able
350 to escape the manipulation of apoptosis by the parasite. In addition, when a study follows
351 mortality across time, the major risk in sampling surviving bees is to artificially select
352 resistant insects with low-level infections or those less sensitive to infection (*e.g.* genetic
353 tendencies). However, even if honeybees are generally stressed by various factors, our study
354 should reveal the metabolic impact of the infection.

355 Finally, other limitations for biological sampling could be the drastic treatments for bee
356 infection, CO_2 anesthesia and hemolymph harvesting. In order to prevent any
357 artificial/technical disruptions, following a rigorous protocol is mandatory ("The

358 Metabolomics Standards Initiative (MSI) and Core Information for Metabolomics Reporting
359 (CIMR),” n.d.).
360
361 ***4.2. Analytical experiments***
362 Discriminating metabolic disturbances is an important issue in metabolomics. Firstly,
363 metabolic coverage, in term of quality and quantity, is strongly linked to analytical tools.
364 Mass spectrometry did not permit easy distinction of isobaric metabolites with similar
365 fragmentation schemes. For this reason, based on our data, it was not possible to distinguish
366 Ile/Leu containing compounds or reveal which hexosamine(s) is (are) impacted. Some NMR
367 signals for ratio calculation were mixed in the same bucket and, thus, polluted. For that
368 reason, they were discarded from our list (e.g. other fructose signals; data not shown). For
369 these reasons, hyphenation using LC-MS, GC-MS and/or NMR is one of the best ways to
370 harvest information, as precisely as possible (Wishart et al., 2008).
371 Secondly, with a very large amount of metabolic signals, data treatments and statistics are
372 required to filter and reveal significant elements before any identification efforts (Monnerie
373 et al., 2019). In our study, combining LC-MS and NMR metabolomics datasets improved
374 coverage of the metabolome. Processing workflows (R packages; (Giacomoni et al., 2015)
375 are time consuming but ensure data reproducibility and comparability. The differences in the
376 metabolome profiles were deciphered using multivariate statistics (PLS-DA). Many statistical
377 tools are able to manage such datasets, but multidimensional representations permit
378 maintenance of data integrity and complexity. Such approach reveals, at the same time, the
379 variability of the complete dataset and the group of signals that are most relevant
380 considering the scientific hypothesis (Boccard and Rudaz, 2014). Analytical redundancy (*e.g.*

hexosamine in MS; Choline and spermidine in NMR) and metabolic interaction are keys for the explanation of such statistical effects and reinforce the identification of biomarkers.

Finally, LC-MS-MS as well as 2D-NMR enhanced the identification of biomarkers. They are low throughput experiments, mostly targeted on the few signals of interest, but increase the quality of the identification. Data mining should be time consuming depending on what kind of metabolite is highlighted. The well-known primary metabolite is quickly identified; those less documented will take time to be identified with certainty. But guessing for "*de novo*" identification (no information in databases) requires high resolution analytical experiments to succeed.

4.3. Biomarkers of the infection and impacts on honeybee metabolism

Because hemolymph is the sole biofluid which circulates in the interior of arthropod body, we can infer that the metabolome of a hemolymph sample reflects the exchanges occurring between organs (digestive, neural, reproductive, etc.) during the infectious process. As expected, the age of bees was the parameter with the strongest effect on the hemolymph metabolome. However, we succeeded in identifying 15 metabolites that were assigned as candidate biomarkers representative of infection alone or the combined effect of age and infection. The levels of these metabolites could be interpreted as either a deleterious impact of infectious process or a defensive response against the pathogen.

The same pattern was observed for O-phosphorylethanolamine (PE), the dipeptide Glu-Leu/Ile, glucose and fructose (α and β forms). These metabolites were more abundant in the hemolymph of infected bees, particularly at D2 post-infection. Glycerophosphocholine (GPC; one major form of choline storage) identified by both LC-MS and NMR, as well as two other dipeptides (Cys-Cys and Glu-Thr), were also increased in infected samples but only at early

405 time of infection (D2). These observations could be related to impacts on proteins as
406 building blocks and glycerophospholipid used in nervous and parasympathic systems.
407 Infection is known to increase energetic demand and modify behavior in *N. ceranae*-infected
408 bees (Alaux et al., 2010a; Martín-Hernández et al., 2011; Mayack and Naug, 2009; Naug and
409 Gibbs, 2009). Some dipeptides also are known to have physiological or cell-signaling effects,
410 although most are simply short-lived intermediates on their way to specific amino acid
411 degradation pathways following further proteolysis. Some recent studies showed that lipid
412 depletion is a phenomenon strongly linked to pathogen development (Franchet et al., 2019;
413 Li et al., 2018). The level of amino acids and spermidine was lower in *Nosema*-exposed
414 samples at D2 post-infection, whereas an antagonistic pattern occurred at D10 between
415 proline and histidine. Decreased levels of amino acids, including proline, were also observed
416 by (Aliferis et al., 2012) in the hemolymph of bees naturally infected by *N. ceranae*.
417 Spermidine seems to be unmodified at D10. Proline and spermidine are involved in a key
418 pathway, the arginine and proline pathway, at the boundary of important metabolisms
419 (amino acids, glutathione, polyamine, etc.). Proline, the dipeptide Glu-Thr and GPC
420 decreased at D10. The level of proline decreased as well in infected bees at D2 while the
421 others increased. Hexosamine, the amino acid histidine and the amino alcohol choline
422 showed a different pattern. The levels of these three metabolites were lower in infected
423 bees at D2 and higher at D10 when compared to uninfected bees. Hexosamine may lead to
424 the biosynthesis of chitin, one of the essential components of insect cuticle and peritrophic
425 matrix in the gut. The peritrophic matrix lines the midgut of most insects and is a protective
426 barrier against microbial infections (Kelkenberg et al., 2015). Chitin is also a major
427 component of the cell wall of microsporidian spores (Bigliardi et al., 1996). Some studies
428 revealed a degeneration of the peritrophic membrane in bees infected by *N. ceranae*

(Dussaubat et al., 2012). Thus, the higher level of hexosamine detected in the hemolymph of infected bees at D10 could be the result of degradation of the peritrophic matrix during the infectious process.

CONCLUSION

This study is the first presenting a complete methodology to analyze bee hemolymph using the up-to-date technologies for metabolomics, MS and NMR. The aim of our study was to detect signatures of the pathological processes during the infection of bees by the gut parasite *N. ceranae*. As a proof of concept, we identified biomarkers that could be useful for a better understanding of pathophysiological mechanisms of the honeybee infection by *N. ceranae.*

For further experiments, we recommend evaluation of the identified biomarkers, through precise quantification, on workers from hives under different field conditions. This untargeted metabolomic approach could also be used to identify biomarkers in the gut during the progression of the infection. In order to reduce disturbances related to other biotic or abiotic factors, we propose to use hives under insect mesh tunnels and follow health status of colonies through random testing.

Acknowledgement:

This work was funded by grants from the French National Research Agency (ANR, grant number ANR-12-BSV3-0020) and received support from PIA METABOHUB (ANR-AA-INSB-0010) and TGIR-RMN (IR-RMN-THC Fr3050 CNRS).

Figure captions

Figure 1. PLS-DA on LC/MS profiles. Batch 1 with 23 analyses (1), Batch 2 with 25 analyses (2). Box for Day 2, dot for Day 10, blue figure for uninfected samples and red for infected ones. A strong age effect is shown on the two batches (dashed black line). (1) PC1 (25,7%) and PC2 (18,3%), (2) PC1 (20,9%) and PC2 (12,4%); Hotelling T2 (ellipse) = 95%.

Figure 2. PLS-DA on NMR data. Box for Day 2, dot for Day 10, blue figure for uninfected samples and red for infected ones. An age effect is shown on the model (dashed black line). PC1 (44,8%) and PC2 (14,1%); Hotelling T2 (ellipse) = 95%.

Table 1: Putative biomarkers identified from LC-MS and MS-MS experiments; ID was obtained from XCMS package (p for positive ionization; first number as mass on charge measurement; T for retention time; second number as the retention time of the ion in minutes). Infected/Uninfected (I/UI) ratios, at two time points (Day 2 and Day 10), were calculated on data matrix (relative intensities). Candidate names were proposed according to data obtained by LC-MS and MS-MS analyses and compared with databases and/or standards. ANOVA filtering distinguished between biomarkers linked to infection only (I) or to both infection and age (II). Signals were identified according to a mass precision less than 1 ppm, except for * 5 ppm far and ** 20 ppm far.

ID	I/UI @ D2	I/UI @ D10	Putative name	ANOVA
p133,058T6,3	0,14	1,55	Aminoacid like	I
p142,03T8,2	1,81	1,40	O-Phosphorylethanolamine	I
p179,054T6,4	0,45	0,63	Carbohydrate like	I
p203,059T5,7	0,42	0,86	Ethyl aconitate **	I
p246,249T5,8	0,84	0,36	Amine like	I
p251.044T6.3	1,17	3,40	Sulfur containing	I
p261,045T7,1	4,75	3,09	γ-Glu-Leu, γ-Glu-Ile	I
p399,134T8,2	2,84	1,67	Short (tri or tetra-) peptide	I
p145,052T5,6	0,36	8,57	Fragment of hexosamine	II
p156,078T8,7	0,52	1,18	Histidine	II
p180,093T5,6	0,38	6,64	Hexosamine	II
p181,092T5,6	0,34	7,26	13C of hexosamine	II
p225,035T6,3	2,38	0,41	Cys-Cys *	II
p249,113T6,9	1,47	0,36	Glu-Thr	II
p280,102T8,3	1,21	0,45	Glycerophosphocholine	II

Table 2: Putative metabolite biomarkers identified from NMR experiments; ID was obtained with AMIX software (the center of each bucket), and Infected/Uninfected (I/UI) ratios, at the two time points (Day 2 and Day 10), were calculated on extracted matrix (relative intensities). Candidate names were proposed according to Identification realized using previously published data and web databases.

ID	I/UI @ D2	I/UI @ D10	Putative name
3.205	0,60	1,16	Choline
3.225	2,04	0,74	GPC
4.005	1,68	1,19	α-Fructose
4.015	1,75	1,17	β-Fructose
4.135	0,81	0,67	Proline
4.115	1,63	1,12	α-Fructose
3.215	1,81	0,82	GPC
3.055	0,84	1,00	Spermidine
1.775	0,85	0,98	Spermidine
1.765	0,87	1,02	Spermidine
3.045	0,84	0,99	Spermidine
5.235	1,15	1,05	α-Glucose
3.195	0,59	1,19	Choline
1.785	0,79	0,95	Spermidine
3.515	0,78	1,10	Choline
3.065	0,85	0,99	Spermidine
4.645	1,12	1,04	β-Glucose

References

Alaux, C., Brunet, J.-L., Dussaubat, C., Mondet, F., Tchamitchan, S., Cousin, M., Brillard, J., Baldy, A., Belzunces, L.P., Conte, Y.L., 2010a. Interactions between Nosema microspores and a neonicotinoid weaken honeybees (Apis mellifera). Environ. Microbiol. 12, 774–782. https://doi.org/10.1111/j.1462-2920.2009.02123.x

Alaux, C., Ducloz, F., Crauser, D., Le Conte, Y., 2010b. Diet effects on honeybee immunocompetence. Biol. Lett. 6, 562–565. https://doi.org/10.1098/rsbl.2009.0986

Alaux, C., Folschweiller, M., McDonnell, C., Beslay, D., Cousin, M., Dussaubat, C., Brunet, J.-L., Conte, Y.L., 2011. Pathological effects of the microsporidium Nosema ceranae on honey bee queen physiology (Apis mellifera). J. Invertebr. Pathol. 106, 380–385. https://doi.org/10.1016/j.jip.2010.12.005

Alaux, C., Sinha, S., Hasadsri, L., Hunt, G.J., Guzmán-Novoa, E., DeGrandi-Hoffman, G., Uribe-Rubio, J.L., Southey, B.R., Rodriguez-Zas, S., Robinson, G.E., 2009. Honey bee aggression supports a link between gene regulation and behavioral evolution. Proc. Natl. Acad. Sci. 106, 15400–15405. https://doi.org/10.1073/pnas.0907043106

Aliferis, K.A., Copley, T., Jabaji, S., 2012. Gas chromatography–mass spectrometry metabolite profiling of worker honey bee (Apis mellifera L.) hemolymph for the study of Nosema ceranae infection. J. Insect Physiol. 58, 1349–1359. https://doi.org/10.1016/j.jinsphys.2012.07.010

Alonso, A., Marsal, S., Julià, A., 2015. Analytical Methods in Untargeted Metabolomics: State of the Art in 2015. Front. Bioeng. Biotechnol. 3. https://doi.org/10.3389/fbioe.2015.00023

Antúnez, K., Martín-Hernández, R., Prieto, L., Meana, A., Zunino, P., Higes, M., 2009. Immune suppression in the honey bee (Apis mellifera) following infection by Nosema ceranae (Microsporidia). Environ. Microbiol. 11, 2284–2290. https://doi.org/10.1111/j.1462-2920.2009.01953.x

Aufauvre, J., Biron, D.G., Vidau, C., Fontbonne, R., Roudel, M., Diogon, M., Viguès, B., Belzunces, L.P., Delbac, F., Blot, N., 2012. Parasite-insecticide interactions: a case study of Nosema ceranae and fipronil synergy on honeybee. Sci. Rep. 2, 1–7. https://doi.org/10.1038/srep00326

Aufauvre, J., Misme-Aucouturier, B., Viguès, B., Texier, C., Delbac, F., Blot, N., 2014. Transcriptome Analyses of the Honeybee Response to Nosema ceranae and Insecticides. PLoS ONE 9. https://doi.org/10.1371/journal.pone.0091686

Bigliardi, E., Selmi, M.G., Lupetti, P., Corona, S., Gatti, S., Scaglia, M., Sacchi, L., 1996. Microsporidian Spore Wall: Ultrastructural Findings on Encephalitozoon hellem Exospore. J. Eukaryot. Microbiol. 43, 181–186. https://doi.org/10.1111/j.1550-7408.1996.tb01388.x

Boccard, J., Rudaz, S., 2014. Harnessing the complexity of metabolomic data with chemometrics. J. Chemom. 28, 1–9. https://doi.org/10.1002/cem.2567

Bundy, J.G., Davey, M.P., Viant, M.R., 2008. Environmental metabolomics: a critical review and future perspectives. Metabolomics 5, 3. https://doi.org/10.1007/s11306-008-0152-0

Chaimanee, V., Chantawannakul, P., Chen, Y., Evans, J.D., Pettis, J.S., 2012. Differential expression of immune genes of adult honey bee (Apis mellifera) after inoculated by Nosema ceranae. J. Insect Physiol. 58, 1090–1095. https://doi.org/10.1016/j.jinsphys.2012.04.016

Chaimanee, V., Warrit, N., Chantawannakul, P., 2010. Infections of Nosema ceranae in four different honeybee species. J. Invertebr. Pathol. 105, 207–210. https://doi.org/10.1016/j.jip.2010.06.005

Chen, Y.-W., Chung, W.-P., Wang, C.-H., Solter, L.F., Huang, W.-F., 2012. Nosema ceranae infection intensity highly correlates with temperature. J. Invertebr. Pathol. 111, 264–267. https://doi.org/10.1016/j.jip.2012.08.014

Cox-Foster, D.L., Conlan, S., Holmes, E.C., Palacios, G., Evans, J.D., Moran, N.A., Quan, P.-L., Briese, T., Hornig, M., Geiser, D.M., Martinson, V., vanEngelsdorp, D., Kalkstein, A.L., Drysdale, A., Hui, J., Zhai, J., Cui, L., Hutchison, S.K., Simons, J.F., Egholm, M., Pettis, J.S., Lipkin, W.I., 2007. A Metagenomic Survey of Microbes in Honey Bee Colony Collapse Disorder. Science 318, 283–287. https://doi.org/10.1126/science.1146498

Dussaubat, C., Brunet, J.-L., Higes, M., Colbourne, J.K., Lopez, J., Choi, J.-H., Martín-Hernández, R., Botías, C., Cousin, M., McDonnell, C., Bonnet, M., Belzunces, L.P., Moritz, R.F.A., Le Conte, Y., Alaux, C., 2012. Gut Pathology and Responses to the Microsporidium Nosema ceranae in the Honey Bee Apis mellifera. PLoS ONE 7. https://doi.org/10.1371/journal.pone.0037017

Dussaubat, C., Maisonnasse, A., Alaux, C., Tchamitchan, S., Brunet, J.-L., Plettner, E., Belzunces, L.P., Le Conte, Y., 2010. Nosema spp. Infection Alters Pheromone Production in Honey Bees (Apis mellifera). J. Chem. Ecol. 36, 522–525. https://doi.org/10.1007/s10886-010-9786-2

Dussaubat, C., Sagastume, S., Gómez-Moracho, T., Botías, C., García-Palencia, P., Martín-Hernández, R., Le Conte, Y., Higes, M., 2013. Comparative study of Nosema ceranae (Microsporidia) isolates from two different geographic origins. Vet. Microbiol. 162, 670–678. https://doi.org/10.1016/j.vetmic.2012.09.012

Fan, T.W.-M., 1996. Metabolite profiling by one- and two-dimensional NMR analysis of complex mixtures. Prog. Nucl. Magn. Reson. Spectrosc. 28, 161–219. https://doi.org/10.1016/0079-6565(95)01017-3

Fiehn, O., 2002. Metabolomics--the link between genotypes and phenotypes. Plant Mol. Biol. 48, 155–171.

Fleming, J.C., Schmehl, D.R., Ellis, J.D., 2015. Characterizing the Impact of Commercial Pollen Substitute Diets on the Level of Nosema spp. in Honey Bees (Apis mellifera L.). PLOS ONE 10, e0132014. https://doi.org/10.1371/journal.pone.0132014

Franchet, A., Niehus, S., Caravello, G., Ferrandon, D., 2019. Phosphatidic acid as a limiting host metabolite for the proliferation of the microsporidium Tubulinosema ratisbonensis in Drosophila flies. Nat. Microbiol. 4, 645–655. https://doi.org/10.1038/s41564-018-0344-y

Fries, I., 2010. Nosema ceranae in European honey bees (Apis mellifera). J. Invertebr. Pathol. 103, S73–S79. https://doi.org/10.1016/j.jip.2009.06.017

Giacomoni, F., Le Corguillé, G., Monsoor, M., Landi, M., Pericard, P., Pétéra, M., Duperier, C., Tremblay-Franco, M., Martin, J.-F., Jacob, D., Goulitquer, S., Thévenot, E.A., Caron, C., 2015. Workflow4Metabolomics: a collaborative research infrastructure for computational metabolomics. Bioinformatics 31, 1493–1495. https://doi.org/10.1093/bioinformatics/btu813

Gisder, S., Hedtke, K., Möckel, N., Frielitz, M.-C., Linde, A., Genersch, E., 2010. Five-Year Cohort Study of Nosema spp. in Germany: Does Climate Shape Virulence and Assertiveness of Nosema ceranae? Appl. Environ. Microbiol. 76, 3032–3038. https://doi.org/10.1128/AEM.03097-09

Goblirsch, M., Huang, Z.Y., Spivak, M., 2013. Physiological and Behavioral Changes in Honey Bees (Apis mellifera) Induced by Nosema ceranae Infection. PLOS ONE 8, e58165. https://doi.org/10.1371/journal.pone.0058165

Goulson, D., Nicholls, E., Botías, C., Rotheray, E.L., 2015. Bee declines driven by combined stress from parasites, pesticides, and lack of flowers. Science 347. https://doi.org/10.1126/science.1255957

Higes, M., Martín, R., Meana, A., 2006. Nosema ceranae, a new microsporidian parasite in honeybees in Europe. J. Invertebr. Pathol. 92, 93–95. https://doi.org/10.1016/j.jip.2006.02.005

Higes, M., Meana, A., Bartolomé, C., Botías, C., Martín-Hernández, R., 2013. Nosema ceranae (Microsporidia), a controversial 21st century honey bee pathogen. Environ. Microbiol. Rep. 5, 17–29. https://doi.org/10.1111/1758-2229.12024

Holt, H.L., Aronstein, K.A., Grozinger, C.M., 2013. Chronic parasitization by Nosema microsporidia causes global expression changes in core nutritional, metabolic and behavioral pathways in honey bee workers (Apis mellifera). BMC Genomics 14, 799. https://doi.org/10.1186/1471-2164-14-799

584 Invernizzi, C., Abud, C., Tomasco, I.H., Harriet, J., Ramallo, G., Campá, J., Katz, H., Gardiol, G.,
585 Mendoza, Y., 2009. Presence of Nosema ceranae in honeybees (Apis mellifera) in Uruguay. J.
586 Invertebr. Pathol. 101, 150–153. https://doi.org/10.1016/j.jip.2009.03.006
587 Kelkenberg, M., Odman-Naresh, J., Muthukrishnan, S., Merzendorfer, H., 2015. Chitin is a necessary
588 component to maintain the barrier function of the peritrophic matrix in the insect midgut.
589 Insect Biochem. Mol. Biol. 56, 21–28. https://doi.org/10.1016/j.ibmb.2014.11.005
590 Kuhl, C., Tautenhahn, R., Böttcher, C., Larson, T.R., Neumann, S., 2012. CAMERA: An integrated
591 strategy for compound spectra extraction and annotation of LC/MS data sets. Anal. Chem.
592 84, 283. https://doi.org/10.1021/ac202450g
593 Kurze, C., Conte, Y.L., Dussaubat, C., Erler, S., Kryger, P., Lewkowski, O., Müller, T., Widder, M.,
594 Moritz, R.F.A., 2015. Nosema Tolerant Honeybees (Apis mellifera) Escape Parasitic
595 Manipulation of Apoptosis. PLOS ONE 10, e0140174.
596 https://doi.org/10.1371/journal.pone.0140174
597 Lankadurai, B.P., Nagato, E.G., Simpson, M.J., 2013. Environmental metabolomics: an emerging
598 approach to study organism responses to environmental stressors. Environ. Rev. 21, 180–
599 205. https://doi.org/10.1139/er-2013-0011
600 Li, W., Chen, Y., Cook, S.C., 2018. Chronic Nosema ceranae infection inflicts comprehensive and
601 persistent immunosuppression and accelerated lipid loss in host Apis mellifera honey bees.
602 Int. J. Parasitol. 48, 433–444. https://doi.org/10.1016/j.ijpara.2017.11.004
603 Liu, X., Locasale, J.W., 2017. Metabolomics: A Primer. Trends Biochem. Sci. 42, 274–284.
604 https://doi.org/10.1016/j.tibs.2017.01.004
605 Martín-Hernández, R., Botías, C., Barrios, L., Martínez-Salvador, A., Meana, A., Mayack, C., Higes, M.,
606 2011. Comparison of the energetic stress associated with experimental Nosema ceranae and
607 Nosema apis infection of honeybees (Apis mellifera). Parasitol. Res. 109, 605–612.
608 https://doi.org/10.1007/s00436-011-2292-9
609 Mayack, C., Naug, D., 2010. Parasitic infection leads to decline in hemolymph sugar levels in
610 honeybee foragers. J. Insect Physiol. 56, 1572–1575.
611 https://doi.org/10.1016/j.jinsphys.2010.05.016
612 Mayack, C., Naug, D., 2009. Energetic stress in the honeybee Apis mellifera from Nosema ceranae
613 infection. J. Invertebr. Pathol. 100, 185–188. https://doi.org/10.1016/j.jip.2008.12.001
614 Medici, S.K., Sarlo, E.G., Porrini, M.P., Braunstein, M., Eguaras, M.J., 2012. Genetic variation and
615 widespread dispersal of Nosema ceranae in Apis mellifera apiaries from Argentina. Parasitol.
616 Res. 110, 859–864. https://doi.org/10.1007/s00436-011-2566-2
617 Monnerie, S., Petera, M., Lyan, B., Gaudreau, P., Comte, B., Pujos-Guillot, E., 2019. Analytic
618 Correlation Filtration: A New Tool to Reduce Analytical Complexity of Metabolomic Datasets.
619 Metabolites 9. https://doi.org/10.3390/metabo9110250
620 Naug, D., Gibbs, A., 2009. Behavioral changes mediated by hunger in honeybees infected with
621 Nosema ceranae. Apidologie 40, 595–599. https://doi.org/10.1051/apido/2009039
622 Nicholson, J.K., Foxall, P.J.D., Spraul, Manfred., Farrant, R.Duncan., Lindon, J.C., 1995. 750 MHz 1H
623 and 1H-13C NMR Spectroscopy of Human Blood Plasma. Anal. Chem. 67, 793–811.
624 https://doi.org/10.1021/ac00101a004
625 Paris, L., El Alaoui, H., Delbac, F., Diogon, M., 2018. Effects of the gut parasite Nosema ceranae on
626 honey bee physiology and behavior. Curr. Opin. Insect Sci., Ecology •
627 Parasites/Parasitoids/Biological control 26, 149–154.
628 https://doi.org/10.1016/j.cois.2018.02.017
629 Pettis, J.S., vanEngelsdorp, D., Johnson, J., Dively, G., 2012. Pesticide exposure in honey bees results
630 in increased levels of the gut pathogen Nosema. Naturwissenschaften 99, 153–158.
631 https://doi.org/10.1007/s00114-011-0881-1
632 Retschnig, G., Neumann, P., Williams, G.R., 2014. Thiacloprid–Nosema ceranae interactions in honey
633 bees: Host survivorship but not parasite reproduction is dependent on pesticide dose. J.
634 Invertebr. Pathol. 118, 18–19. https://doi.org/10.1016/j.jip.2014.02.008

Simón-Manso, Y., Lowenthal, M.S., Kilpatrick, L.E., Sampson, M.L., Telu, K.H., Rudnick, P.A., Mallard, W.G., Bearden, D.W., Schock, T.B., Tchekhovskoi, D.V., Blonder, N., Yan, X., Liang, Y., Zheng, Y., Wallace, W.E., Neta, P., Phinney, K.W., Remaley, A.T., Stein, S.E., 2013. Metabolite Profiling of a NIST Standard Reference Material for Human Plasma (SRM 1950): GC-MS, LC-MS, NMR, and Clinical Laboratory Analyses, Libraries, and Web-Based Resources. Anal. Chem. 85, 11725–11731. https://doi.org/10.1021/ac402503m

The Metabolomics Standards Initiative (MSI) and Core Information for Metabolomics Reporting (CIMR) [WWW Document], n.d. URL msi.html (accessed 3.10.20).

vanEngelsdorp, D., Evans, J.D., Saegerman, C., Mullin, C., Haubruge, E., Nguyen, B.K., Frazier, M., Frazier, J., Cox-Foster, D., Chen, Y., Underwood, R., Tarpy, D.R., Pettis, J.S., 2009. Colony Collapse Disorder: A Descriptive Study. PLOS ONE 4, e6481. https://doi.org/10.1371/journal.pone.0006481

vanEngelsdorp, D., Meixner, M.D., 2010. A historical review of managed honey bee populations in Europe and the United States and the factors that may affect them. J. Invertebr. Pathol. 103, S80–S95. https://doi.org/10.1016/j.jip.2009.06.011

Vidau, C., Diogon, M., Aufauvre, J., Fontbonne, R., Viguès, B., Brunet, J.-L., Texier, C., Biron, D.G., Blot, N., El Alaoui, H., Belzunces, L.P., Delbac, F., 2011. Exposure to Sublethal Doses of Fipronil and Thiacloprid Highly Increases Mortality of Honeybees Previously Infected by Nosema ceranae. PLoS ONE 6. https://doi.org/10.1371/journal.pone.0021550

Wang, L., Meeus, I., Rombouts, C., Meulebroek, L.V., Vanhaecke, L., Smagghe, G., 2019. Metabolomics-based biomarker discovery for bee health monitoring: A proof of concept study concerning nutritional stress in Bombus terrestris. Sci. Rep. 9, 1–11. https://doi.org/10.1038/s41598-019-47896-w

Williams, G.R., Sampson, M.A., Shutler, D., Rogers, R.E.L., 2008. Does fumagillin control the recently detected invasive parasite Nosema ceranae in western honey bees (Apis mellifera)? J. Invertebr. Pathol. 99, 342–344. https://doi.org/10.1016/j.jip.2008.04.005

Willker, W., Engelmann, J., Brand, A., Liedfritz, D., 1996. Metabolite Identification in Cell Extracts and Culture Media by Proton-detected D-H, C-NMR Spectroscopy1. J. Magn. Reson. Anal. 21–32.

Wishart, D.S., Lewis, M.J., Morrissey, J.A., Flegel, M.D., Jeroncic, K., Xiong, Y., Cheng, D., Eisner, R., Gautam, B., Tzur, D., Sawhney, S., Bamforth, F., Greiner, R., Li, L., 2008. The human cerebrospinal fluid metabolome. J. Chromatogr. B Analyt. Technol. Biomed. Life. Sci. 871, 164–173. https://doi.org/10.1016/j.jchromb.2008.05.001

Wu, J.Y., Smart, M.D., Anelli, C.M., Sheppard, W.S., 2012. Honey bees (Apis mellifera) reared in brood combs containing high levels of pesticide residues exhibit increased susceptibility to Nosema (Microsporidia) infection. J. Invertebr. Pathol. 109, 326–329. https://doi.org/10.1016/j.jip.2012.01.005

Zhang, A., Sun, H., Wu, X., Wang, X., 2012. Urine metabolomics. Clin. Chim. Acta 414, 65–69. https://doi.org/10.1016/j.cca.2012.08.016

Zhang, X., Li, Q., Xu, Z., Dou, J., 2020. Mass spectrometry-based metabolomics in health and medical science: a systematic review. RSC Adv. 10, 3092–3104. https://doi.org/10.1039/C9RA08985C

Zhao, X., Fritsche, J., Wang, J., Chen, J., Rittig, K., Schmitt-Kopplin, P., Fritsche, A., Häring, H.-U., Schleicher, E.D., Xu, G., Lehmann, R., 2010. Metabonomic fingerprints of fasting plasma and spot urine reveal human pre-diabetic metabolic traits. Metabolomics 6, 362–374. https://doi.org/10.1007/s11306-010-0203-1

Web references

« Human Metabolome Database ». https://hmdb.ca/.

« KEGG: Kyoto Encyclopedia of Genes and Genomes ». https://www.genome.jp/kegg/.

« MassBank | MSSJ MassBank Mass Spectral DataBase ». http://www.massbank.jp/.

« PRIMe: Platform for RIKEN Metabolomics ».
http://prime.psc.riken.jp/?action=standard_index.

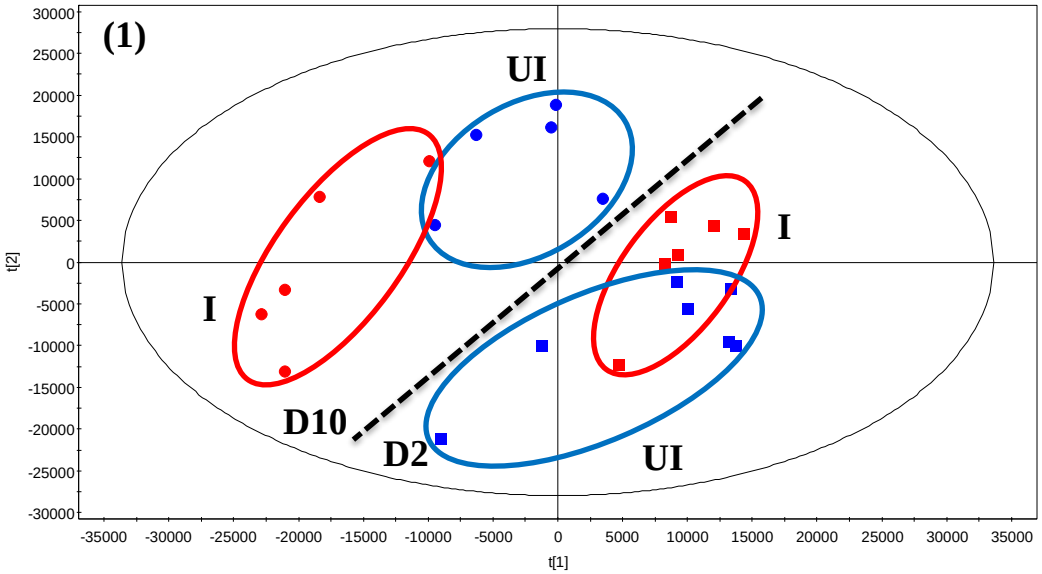

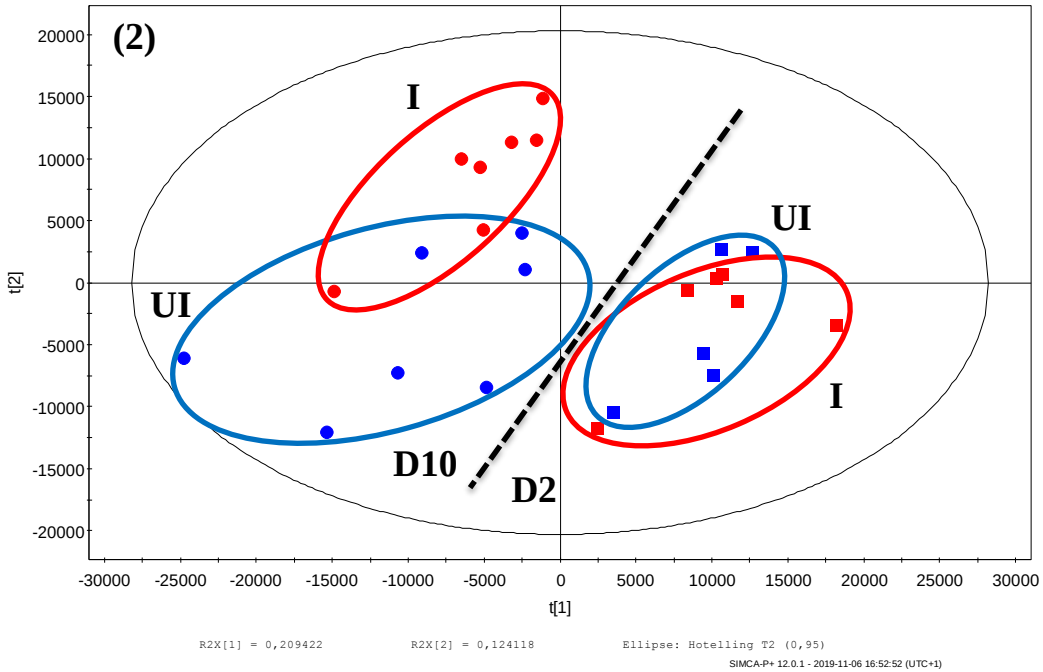

Fig.1: PLS-DA on LC/MS profiles.

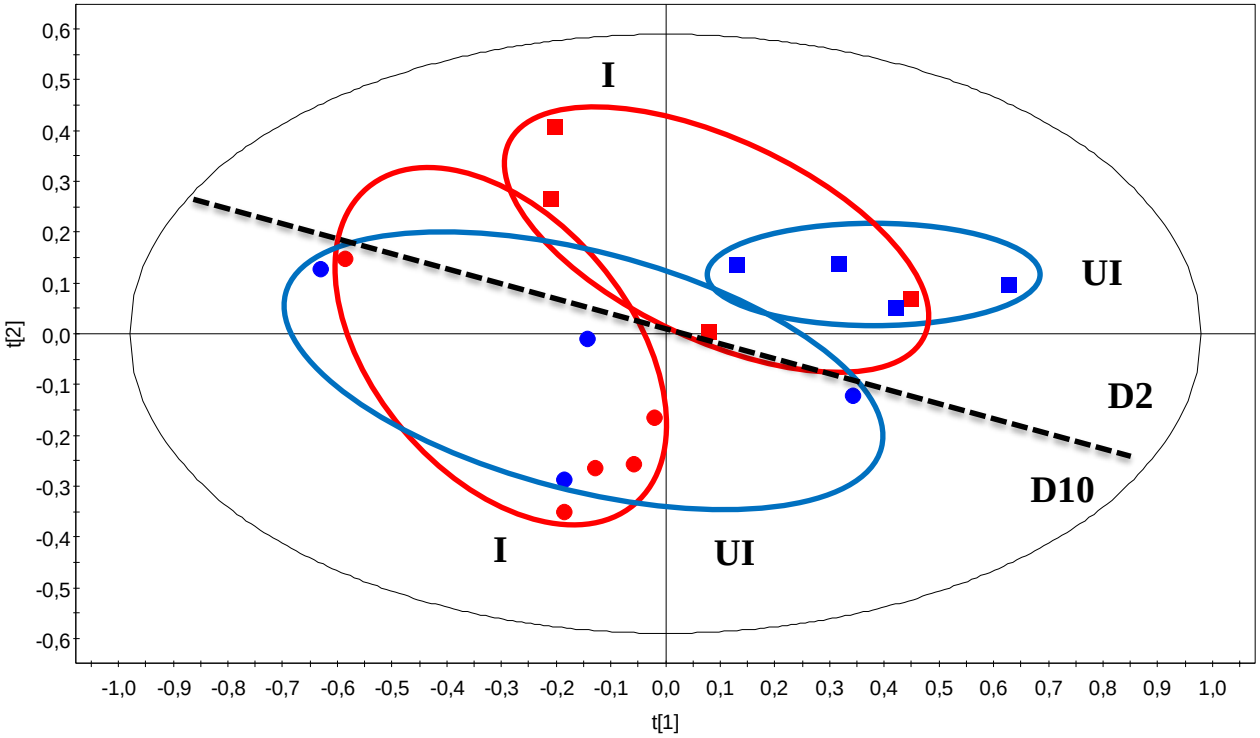

Fig.2: PLS-DA on NMR data.

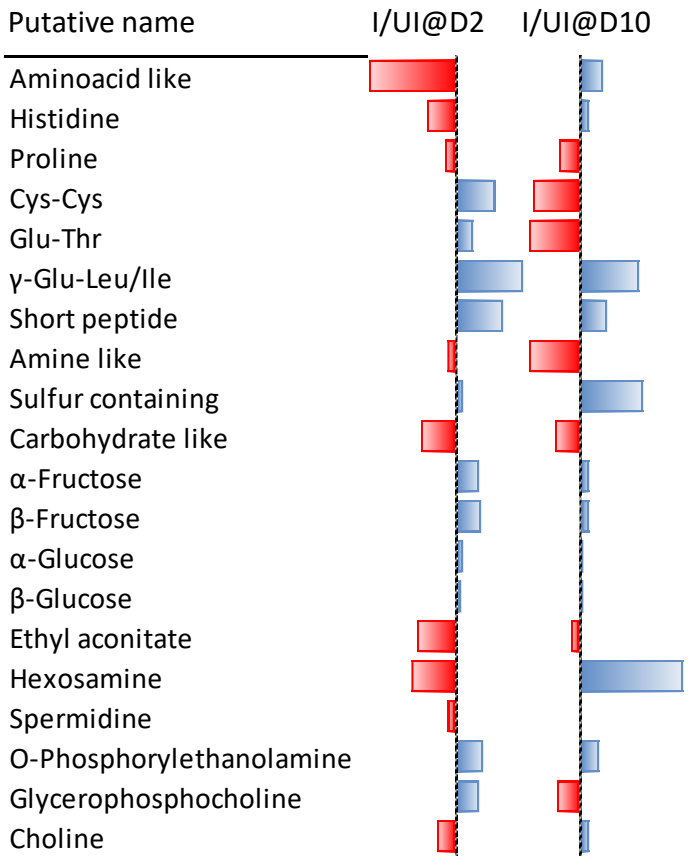
Putative name
I/UI@D2
I/UI@D10
Aminoacid like
Histidine
Proline
Cys-Cys
Glu-Thr
γ-Glu-Leu/Ile
Short peptide
Amine like
Sulfur containing
Carbohydrate like
α-Fructose
β-Fructose
α-Glucose
β-Glucose
Ethyl aconitate
Hexosamine
Spermidine
O-Phosphorylethanolamine
Glycerophosphocholine
Choline